

# Comparative study of different theories on active earth pressure

S. P. Yap, F. A. Salman, S. M. Shirazi

Department of Civil Engineering, Faculty of Engineering, University of Malaya, Kuala Lumpur 50603, Malaysia

© Central South University Press and Springer-Verlag Berlin Heidelberg 2012

**Abstract:** Determination of distribution and magnitude of active earth pressure is crucial in retaining wall designs. A number of analytical theories on active earth pressure were presented. Yet, there are limited studies on comparison between the theories. In this work, comparison between the theories with finite element analysis is done using the PLAXIS software. The comparative results show that in terms of distribution and magnitude of active earth pressure, RANKINE's theory possesses the highest match to the PLAXIS analysis. Parametric studies were also done to study the responses of active earth pressure distribution to varying parameters. Increasing soil friction angle and wall friction causes decrease in active earth pressure. In contrast, active earth pressure increases with increasing soil unit weight and height of wall. RANKINE's theory has the highest compatibility to finite element analysis among all theories, and utilization of this theory leads to proficient retaining wall design.

**Key words:** active earth pressure; retaining wall; PLAXIS; comparative study; RANKINE's theory; COULOMB's theory

## 1 Introduction

Major concern in retaining wall analysis and design is the determination of magnitude and distribution of lateral earth pressure (active and passive) on the retaining wall. In retaining wall problems, active earth pressure contributes to the failure of the wall. Determination of active earth pressure distribution is a very important step in analysis of a retaining wall and subsequently in its design. Conventional theories from RANKINE and COULOMB are widely used in retaining wall design to calculate magnitude and distribution of active earth pressure [1–2]. However, the linear distribution of the active earth pressure assumed by RANKINE and COULOMB has been pointed out by TERZAGHI [3] and ROSCOE [4] to be inaccurate. Distribution of active earth pressure is non-linear and maximum active earth pressure does not occur at toe of the wall. Therefore, further researches were focused on obtaining the non-linear distribution of active earth pressure by incorporating arching effect [5–8]. Arching is a condition where stress redistribution of a part of soil mass with higher stress to a soil mass with lower stress [9].

DUBROVA [5] is among the early researchers who incorporate arching effect into distribution of active earth pressure. She considered that the wall rotates at the midheight. The disadvantage of DUBROVA's method is that it provides only solution for straight surfaces but

cannot be used for slope surfaces [10]. ROSCOE [4] pointed out that DUBROVA's method to determine earth pressure distribution considering translational mode of wall displacement is open for criticism.

WANG [6] proposed an analytical method to determine a theoretical result for the earth pressure on a retaining wall on the basis of COULOMB's theory. WANG's earth pressure is curvilinearly distributed. PAIK and SALGADO [7] pointed out that WANG's formulation gives a total active force equal to that calculated by COULOMB's theory. However, in reality, COULOMB's solution for total active force is not exact. According to WANG [6], the coefficient of lateral earth pressure,  $K$ , should be between the coefficient of active earth pressure,  $K_a$ , and coefficient of earth pressure at-rest,  $K_o$ , and thus further investigation is needed. But no further discussion is provided by WANG.

PAIK and SALGADO [7] assumed that translational movement of wall and linear failure plane which has an angle of  $45^\circ + \phi/2$  to the horizontal. They checked the accuracy of the new coefficient of active earth pressure developed with the value of new active lateral stress ratio proposed by PAIK and SALGADO [7], and KAWN matches the values of RANKINE's active earth pressure coefficient for  $\delta=0$  (smooth wall). Other than that, they compared their theory with other theories. It is shown that PAIK and SALGADO's method [7] matches the experimental results with better compatibility than other theories.

GOEL and PATRA's theory [8] is an improvement of PAIK and SALGADO's method [5]. They concluded that planar failure surface with parabolic arch shape predicts closest to the experimental results, instead of circular arch assumed by PAIK and SALGADO [7]. They compared their results to that of PAIK and SALGADO [7] and showed that their theory was more accurate.

Other than the analytical theories discussed, different numerical methods are available to determine the distribution of lateral earth pressure. The methods are SOKOLOVSKI's method [11] and Smear Shear Band Method by HAZARIKA and MATSUZAWA [10]. However, the famous numerical method to be used is the finite element analysis.

An accurate distribution of active earth pressure enables an efficient design of retaining wall which reduces the chance of over or underdesign of the walls. An overdesign of a retaining wall will lead to wastage of construction materials whereas an underdesign will lead to a higher risk of failure. Hence, there is a necessity to determine the most accurate theory to be used in retaining wall design. Different theories are available in solving retaining wall problems. However, there are limited studies on comparing these theories for their accuracy or fallacy in determining the active earth pressure. In this work, analytical theories are studied in order to compare these theories. Besides, numerical modeling using PLAXIS software is conducted to check the accuracy of the theories. The well-established PLAXIS as finite element analysis software has its advantages to represent the actual behavior of active earth pressure distribution. In addition, YANG and LIU [12] verified their PLAXIS model by comparing to centrifuge tests documented by FRYDMAN and KEISSAR [13] and TAKE and VALSANGKAR [14] and this enhances the feasibility of PLAXIS in showing the accuracy of numerical modeling. Comparison between finite element analysis and analytical theories shows the compatibility of the theories to the actual behavior of active earth pressure. SALMAN et al [15] had also compared RANKINE, COULOMB and DUBROVA's theories to finite element analysis using a different finite element computer program, CRISP. Other than application in retaining wall design, an efficient determination of active earth pressure aids in solving other related problems like in seismic characteristics as studied by LIN et al [16].

Of course there are many other theories proposed to understand the earth pressure distribution and its effect on the behavior of retaining walls (i.e. YANG [17], EVANGELISTA et al [18] and ZHU et al [19]). Only limited theories can be presented here. The authors tried to focus on the most well-known and used theories.

RANKINE and COULOMB present the classical theories, whereas DUBROVA is the first one who incorporates the arching effect into derivation of the active earth pressure.

## 2 Methodology: Numerical modeling using PLAXIS

Finite element analysis is one of the most accurate numerical methods to find an approximate solution for engineering problems. In short, finite element analysis creates partial differential equations to be solved numerically. With the aid of finite element software which can perform high number of iterations, the accuracy of finite element analysis approximately matches the actual condition of retaining wall problems.

In this work, numerical modeling using PLAXIS 8.2 (denoted as PLAXIS in later discussions) is conducted in order to compare the analytical theories to the finite element analysis and to carry out parametric studies. Table 1 and Fig. 1 show the parameters and geometries used in PLAXIS modeling. The model presented by YANG and LIU [12] is referred with some modifications.

**Table 1** Parameters used for numerical modeling of retaining wall using PLAXIS

Item	Parameter	Control value
Soil properties	Soil unit weight (Dry)/(kN·m <sup>-3</sup> )	16.4
	Friction angle, $\phi$ (°)	36
	Cohesion, $c$ (kN·m <sup>-2</sup> )	0
	Elastic modulus, $E$ (kN·m <sup>-2</sup> )	30 000
	Poisson ratio, $\nu$	0.3
	$R_{inter}$	0.667
Material properties for retaining wall	Bending stiffness, $E_I$ (kN·m <sup>-2</sup> )	$2.5 \times 10^6$
	Normal stiffness, $E_A$ (kN·m <sup>-2</sup> )	$3 \times 10^7$
Geometrical inputs for retaining wall	Height of wall, $H$ /m	5
	Width of backfill, $L$ /m	10
	Fixities	Vertical fixity at toe of wall
	Prescribed displacement	0

## 3 Results and discussion

### 3.1 Distribution of active earth pressure

Distribution of active earth pressure is non-linear and maximum pressure does not occur at the bottom of the wall (Fig. 2). Therefore, the results verify the statement made by GOEL and PATRA [8]. They stated that the assumption by RANKINE and COULOMB

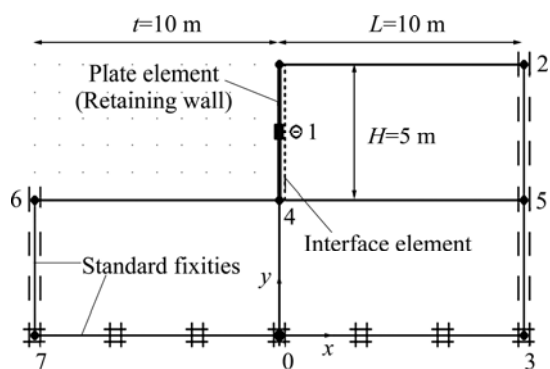


Fig. 1 PLAXIS model for comparison between different theories on active earth pressure and FEA

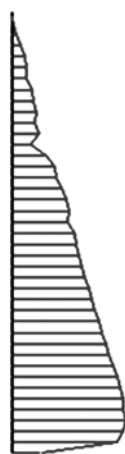


Fig. 2 Distribution of active earth pressure of PLAXIS model

assuming a planar failure surface regardless of wall friction puts maximum pressure at the base of the wall, which underestimates the height of the center of pressure. While TERZAGHI [9] assumed that the failure surface is approximately parabolic in nature and zero stress occurs at the base of the wall, explained by partial support of the soil arching.

### 3.2 Comparison of analytical theories with PLAXIS modeling

Figure 3 shows a graph combining all analytical theories on active earth pressure [1–2, 5–8] and PLAXIS analyses including the present work and YANG and LIU’s analysis [12]. From Fig. 3, the following conclusions can be made:

- 1) The distribution of active earth pressure is linear at the upper midheight of the wall (from top of the wall to 50% of wall height). This matches the results from all analytical theories except GOEL and PATRA [8]. GOEL and PATRA’s theory gives higher active earth pressure than the present work at the upper midheight of the wall.
- 2) For the lower midheight of the wall, the distribution of active earth pressure is non-linear. From 50% to 80% of wall height, the distribution of active earth pressure matches to RANKINE’s theory and

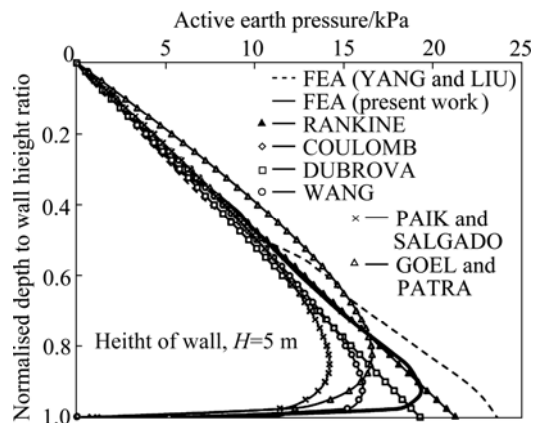


Fig. 3 Different theories and PLAXIS analysis on active earth pressure (NOTE: Results from Coulomb’s theory overlapped with Dubrova’s theory)

remains linear. Therefore, it can be concluded that up to 80% of wall height, most of the distribution of active earth pressure matches to RANKINE’s theory, followed by other theories. After 80% of wall height, the distribution of active earth pressure becomes parabolic until the bottom of the wall (100% of wall height). For this portion, theories presented by COULOMB [1–2], DUBROVA [5], WANG [6], PAIK and SALGADO [7] and GOEL and PATRA [8] give lower active earth pressure than the present work, and only RANKINE’s theory [1–2] shows the most compatible results to the PLAXIS analysis than the other theories. Even though RANKINE’s theory is one of the most conventional theories and its linear distribution has been pointed out by TERZAGHI [3] as a fallacy. However, from PLAXIS analysis, the compatibility of magnitude of RANKINE’s theory in active earth pressure to FEA has proven its effectiveness to be used widely in retaining wall problems. Therefore, it can be concluded that RANKINE’s theory gives the most accurate results compared to the other theories for both magnitude and distribution of active earth pressure.

3) For other theories except RANKINE’s theory, the increasing order of degree of compatibility to FEA is COULOMB [1–2], DUBROVA [5], GOEL and PATRA [8], WANG [6], and PAIK and SALGADO [7].

4) The height of application of maximum active earth pressure of PLAXIS analysis is within the range of 90% to 100% of wall height. From Fig. 3, result from WANG’s theory falls under this range as well, but with lower magnitude of maximum active earth pressure. After that, maximum active earth pressure from PAIK and SALGADO [7] is slightly higher than the PLAXIS result. Result from GOEL and PATRA [8] shows the highest deviation from PLAXIS result, at which its height of application of maximum active earth pressure is located in the range of 80% to 90% of wall height. Finally, for theories of RANKINE, COULOMB [1–2]

and DUBROVA [5], the maximum active earth pressure is located at the bottom of the wall. Therefore, it can be concluded that WANG's method provides the most compatible result to FEA for height of application of maximum active earth pressure.

### 3.3 Parametric studies

#### 3.3.1 Soil friction angle

The first parametric study is carried out on varying soil friction angle,  $\phi$ , by using the same model used in previous section. From Table 1, the soil friction angle used in previous section is  $36^\circ$ , similar to the results of YANG and LIU [12]. Therefore, model of  $\phi=36^\circ$  is used as the control model in this parametric study. The values of  $\phi$  used in this part are  $0^\circ$ ,  $10^\circ$ ,  $20^\circ$ ,  $30^\circ$ ,  $36^\circ$ , and  $40^\circ$ . The case of  $\phi=0$  represents liquid behavior of the soil. Figure 4 shows the distribution of active earth pressure for different  $\phi$ .

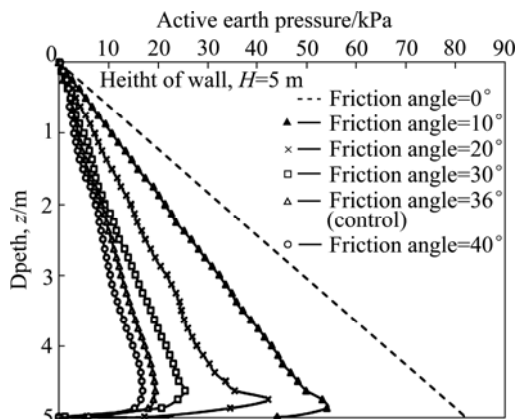


**Fig. 4** Change of active earth pressure distribution with depth at different friction angles

From Fig. 4, when the friction angle increases from  $\phi=0$ , the distribution of active earth pressure changes from linear to non-linear. For  $\phi=0$ , the distribution of active earth pressure is linear with the highest value located at the bottom of wall. For this case, there is no shear strength in the soil (zero cohesion and zero friction angle). Therefore, in liquid condition, the soil does not provide resistance to shear, and the active earth pressure is directly proportional to the vertical stress acting on the soil. This leads to a linear distribution of active earth pressure as shown in Fig. 4.

As the friction angle increases, the active pressure acting on every depth of the retaining wall decreases and the height of application of the maximum active earth pressure (towards top of the wall) increases. This is due to the increasing internal shear strength within the soil with increasing soil friction angle. Hence, less active earth pressure can develop. The lowest active earth pressure and highest height of application of the maximum active earth pressure (towards top of the wall) are observed in case  $\phi=40^\circ$ . Moreover, when the soil

friction angle is larger than  $30^\circ$ , the difference in distribution of active earth pressure is less when soil friction angle changes, compared to soil friction angles less than  $30^\circ$ . These changes in response to varying in values of  $\phi$  match the parametric study carried out by PAIK and SALGADO [7].

#### 3.3.2 Soil unit weight

The second parametric study is carried out on varying soil unit weight,  $\gamma$ . Similar to the first parametric study, PLAXIS model in previous section with unit weight of  $16.4 \text{ kN/m}^3$  is used as control model. Distribution of active earth pressure with varying unit weight is shown in Fig. 5. In this parametric study, the unit weights used are 12, 15, 16.4 and  $18 \text{ kN/m}^3$ .

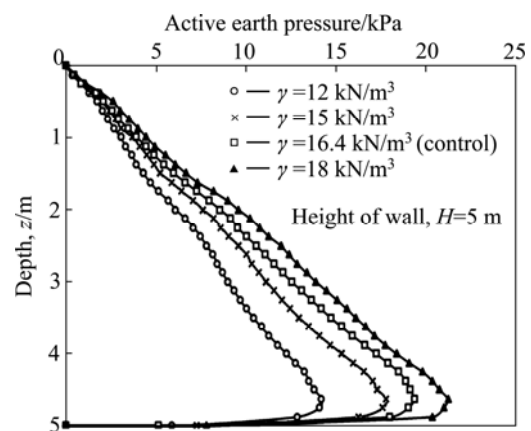


**Fig. 5** Graph of active earth pressure with depth with different soil unit weights

From Fig. 5, the active earth pressure acting on each depth throughout the retaining wall increases with increasing the soil unit weight. This situation matches the previous discussion at which soil with a higher unit weight will exert a higher active earth pressure on the retaining wall. Next, the height of application of maximum active earth pressure (towards top of the wall) does not change significantly in response to the change in soil unit weight. Refer to Fig. 5, when soil unit weight increases, the height of application of active earth pressure increases with a very small amount of depth towards the top of the wall only.

When soil unit weight increases, vertical stress acting on a soil mass increases, and eventually causes lateral active stress to increase. Moreover, soil with higher unit weight requires a less wall displacement for development of active earth pressure [2]. Therefore, this can be explained that when soil unit weight increases, the active earth pressure acting on retaining wall increases.

#### 3.3.3 Height of wall

The varied parameter in the third parametric study is height of wall,  $H$ . In control model from previous section, the height of wall used is 5 m. In this parametric study, the values of height of wall used are 4, 5 and 6 m. Figure 6 shows the results from PLAXIS analysis.

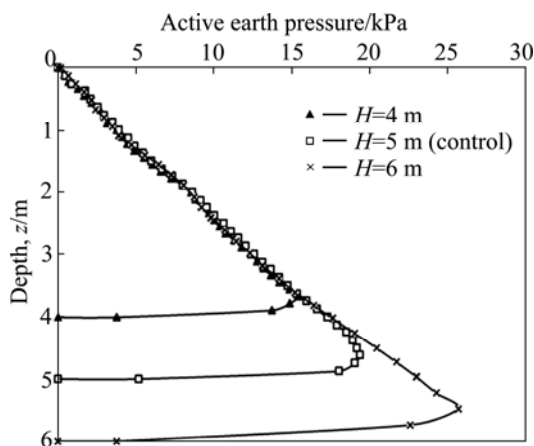


**Fig. 6** Graph of active earth pressure with depth at different heights of wall

From Fig. 6, the height of wall does not affect the shape of the distribution of active earth pressure, but has effect on its magnitude. For the shape of active earth pressure distribution, the distribution remains linear and has similar magnitude along the whole height of retaining wall except the last half meter from bottom of the wall. This means that the linear portion of distribution of active earth pressure occurs at top 3.5 m for 4 m wall, at top 4.5 m for 5 m wall and at top 5.5 m for 6 m wall. In the last half meter of the wall height, the distribution of active earth pressure is in parabolic shape, and magnitude increases for increasing wall height.

The results match to parametric study of PAIK and SALGADO [7], as shown in Fig. 7. From Fig. 7, distribution of active earth pressure increases at every normalized depth to wall height ratio ( $z/H$ ) when the height of wall increases.

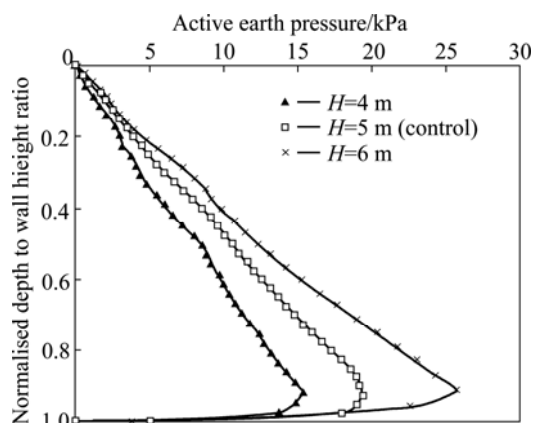


**Fig. 7** Change of active earth pressure distribution with normalised depth to wall height ratio

### 3.3.4 Wall friction

The fourth parametric study is carried out on the wall friction,  $\delta$ , or in other words, the friction angle between the soil and the retaining wall. In this parametric study, the wall friction used is  $26^\circ$ , which gives a  $R_{inter}$

value of 0.667, as given by YANG and LIU [12]. All values for wall friction used in this parametric study are  $0^\circ, 10^\circ, 20^\circ, 26^\circ$ , and  $36^\circ$ . The results are shown in Fig. 8.

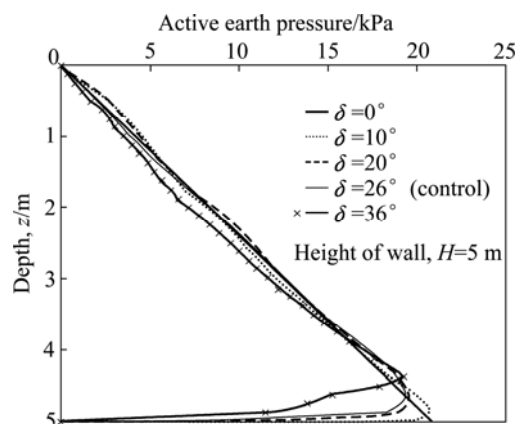


**Fig. 8** Graph of active earth pressure with depth at different friction angles

Referred to Fig. 8, for smooth wall ( $\delta=0$ ), the distribution of active earth pressure is linear, which is consistent to RANKINE's theory. As the wall friction increases, the distribution of active earth pressure changes from linear (for  $\delta=0$ ) to non-linear. At upper zone of the wall, the magnitude of active earth pressure is almost equal to the minimum deviation as wall friction increases. While for lower zone of the wall (which includes 0.5 m from bottom of the wall), as the wall friction increases, both the maximum active earth pressure the and height of application of maximum active earth pressure towards the top of wall increase.

### 3.4 Effect of cohesion

Another PLAXIS model (denoted as Model II) is done with reference to YANG and LIU [12] in order to investigate the effect of cohesion on the distribution of active earth pressure. In Model II, cohesion of  $1 \text{ kN/m}^2$  is used. From the results shown in Fig. 9, when cohesion

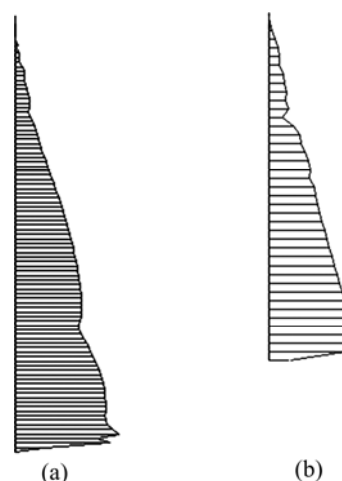


**Fig. 9** Comparison of active earth pressure on (a) Model II and (b) PLAXIS model

exists within the soil, a zone with zero active earth pressure occurs at the top of the wall. The result matches with tensile crack zone given by RANKINE and COULOMB [1].

### 3.5 Effective normal stress, bending moment, shear force and total displacement of retaining wall

Figure 10 shows the different forces acting on the retaining wall and total displacement of retaining wall in Model II. These results are important for design of retaining wall. Figure 10(a) shows the distribution of active earth pressure acting on the retaining wall, denoted as effective normal stresses acting on the retaining wall in PLAXIS output. While Figs. 10(b) and (c) show the bending moment and shear force of the retaining wall, respectively. From Fig. 10 (b), the maximum bending moment is located at the middle height of the retaining wall. Hence, for retaining wall designs, the middle height zone has to be designed to support high bending moment and decrease the bending moment near top and bottom of the wall. In other words, the highest reinforcement must be located near the middle height for reinforced concrete retaining walls. While from Fig. 10(c), the highest shear forces are located at the quarter-height from top of the wall and near bottom of the wall. Therefore, high shear reinforcement has to be applied at these zones for reinforced concrete retaining walls.

The total displacement of retaining wall is shown in

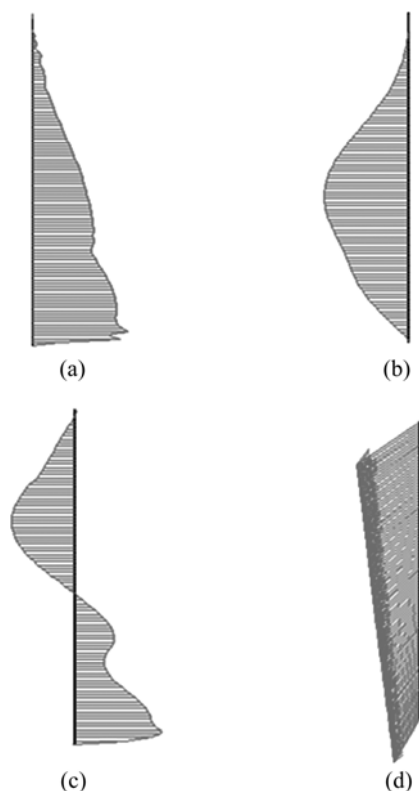


**Fig. 10** (a) Effective normal stress, (b) bending moment, (c) shear force, and (d) total displacement of retaining wall

Fig. 10(d). The direction of displacement of the wall is the same as the rotation at the bottom of wall. In addition, the magnitude of the total displacement is only 2.31 mm, which is very small.

## 4 Conclusions

1) From the comparison of active earth pressure calculated from analytical theories and finite element analysis, results from RANKINE's theory show the highest compatibility to the PLAXIS analysis, for the magnitude and distribution of active earth pressure.

2) While in parametric studies, when soil friction angle and wall friction increase, the active earth pressure decreases. On the other hand, when the soil unit weight and height of wall increase, the active earth pressure increases.

3) For cohesive soil, the tension zone with zero active earth pressure exists at top of retaining wall.

4) The maximum bending moment occurs at midheight of the retaining wall while the maximum shear force is observed at the quarter-height at the top and bottom of the wall.

5) Utilization of the most accurate theory, which is RANKINE's theory as proven in this study, can lead to efficient retaining wall designs.

## Acknowledgement

The authors would like to acknowledge and extend gratitude to the University of Malaya for the encouragement, technical support, and especially for the financial support by the Institute of Research Management and Monitoring (IPPP), University of Malaya (UM) under UMRG grant number (RG086/10AET).

## References

- [1] DAS B M. Principles of foundation engineering [M]. 7th ed. Singapore: International Thomson Publishing Asia, 2010.
- [2] BOWLES J E. Foundation analysis and design [M]. 5th ed. Singapore, McGraw-Hill, 1996.
- [3] TERZAGHI K. A fundamental fallacy in earth pressure computations [J]. Journal of Boston Society of Civil Engineers, 1936, 23: 71–88.
- [4] ROSCOE K H. The influence of strains in soil mechanics [J]. Geotechnique, 1970, 20(2): 129–170.
- [5] DUBROVA G A. Intersection of soil and structures [M]. Moscow, Izd. Rechnoy Transport, 1963.
- [6] WANG Y Z. Distribution of earth pressure on a retaining wall [J]. Geotechnique, 2000, 50(1): 83–88.
- [7] PAIK K H, SALGADO R. Estimation of active earth pressure against rigid retaining walls considering arching effects [J]. Geotechnique, 2003, 53(7): 643–653.
- [8] GOEL S, PATRA N R. Effect of arching on active earth pressure for rigid retaining walls considering translation mode [J]. International Journal of Geomechanics, 2008, 8(2): 123–133.
- [9] TERZAGHI K. Theoretical soil mechanics [M]. New York: John

- Wiley and Sons, 1954.
- [10] HAZARIKA H, MATSUZAWA H. Wall displacement modes dependant active earth pressure analyses using shear band method with two bands [J]. *Computer and Geotechnics*, 1996, 19(3): 193–219.
- [11] SOKOLOVSKI V V. *Statics of soil media* [M]. 2nd ed. London: Butterworths Scientific Publications, 1960.
- [12] YANG Kuo-hsin, LIU Chia-nan. Finite element analysis of earth pressures for narrow retaining walls [J]. *Journal of GeoEngineering*, 2007, 2(2): 43–52.
- [13] FRYDMAN S, KEISSAR I. Earth pressure on retaining walls near rock faces [J]. *Journal of Geotechnical Engineering: ASCE*, 1987, 113(6): 586–599.
- [14] TAKE W A, VALSANGKAR A J. Earth pressure on unyielding retaining walls of narrow backfill width [J]. *Canadian Geotechnical Journal*, 2001, 38: 1220–1230.
- [15] SALMAN F A, AL-SHKARCHI Y J, HUSAIN H M, SABRE D K. Distribution of earth pressure behind retaining walls considering different approaches [J]. *International Journal of the Physical Sciences*, 2010, 5(9): 1389–1400.
- [16] LIN Yu-lian, LIU Yong-jian, LI Jia-le. Dynamic response law about gravity retaining wall to seismic characteristics and earth fill properties [J]. *Journal of Central South University*, 2012, 19(3): 657–663.
- [17] YANG Xiao-li. Upper bound limit analysis of active earth pressure with different fracture surface and nonlinear yield criterion [J]. *Theoretical and Applied Fracture Mechanics*, 2007, 47: 46–56.
- [18] EVANGELISTA A, SANTOLO A S D, SIMONELLI A L. Evaluation of pseudostatic active earth pressure coefficient of cantilever retaining walls [J]. *Soil Dynamics and Earthquake Engineering*, 2010, 30: 1119–1128.
- [19] ZHU Jian-feng, XU Ri-qing, LI Xin-rui, CHEN Ye-kai. Calculation of earth pressure based on disturbed state concept theory [J]. *Journal of Central South University of Technology*, 2011, 18(4): 1240–1247.

(Edited by HE Yun-bin)